European Journal of Pharmaceutics and Biopharmaceutics 78 (2011) 83–89

Contents lists available at ScienceDirect

European Journal of Pharmaceutics and Biopharmaceutics

journal homepage: www.elsevier.com/locate/ejpb

Research paper

Modelling of molecular phase transitions in pharmaceutical inhalation compounds: An *in silico* approach

Heba Abdel-Halim [a], Daniela Traini [a], David Hibbs [a], Simon Gaisford [b], Paul Young [a,*]

[a] Faculty of Pharmacy, The University of Sydney, Sydney, Australia
[b] The School of Pharmacy, University of London, London, UK

ARTICLE INFO

Article history:
Received 23 June 2010
Accepted in revised form 13 December 2010
Available online 21 December 2010

Keywords:
Amorphous
Beclomethasone dipropionate
Glass transition temperature
Molecular dynamic simulations

ABSTRACT

Molecular dynamic simulations have been successfully utilised with molecular modelling to estimate the glass transition temperature (T_g) of polymers. In this paper, we use a similar approach to predict the T_g of a small pharmaceutical molecule, beclomethasone dipropionate (BDP). Amorphous beclomethasone dipropionate was prepared by spray-drying. The amorphous nature of the spray-dried material was confirmed with scanning electron microscopy, differential scanning calorimetry (DSC) and X-ray powder diffraction (XRD). Molecular models for amorphous BDP were constructed using the amorphous cell module in Discovery studio™. These models were used in a series of molecular dynamic simulations to predict the glass transition temperature. The T_g of BDP was determined by isothermal-isobaric molecular dynamic simulations, and different thermodynamic parameters were obtained in the temperature range of −150 to 400 °C. The discontinuity at a specific temperature in the plot of temperature versus amorphous cell volume (V) and density (ρ) was considered to be the simulated T_g. The predicted T_g from four different simulation runs was 63.8 °C ± 2.7 °C. The thermal properties of amorphous BDP were experimentally determined by DSC and the experimental T_g was found to be ~65 °C, in good agreement with computational simulations.

1. Introduction

One of the most important properties of an active pharmaceutical ingredient (API) is the polymorphic form, since it directly affects both formulation and drug bioavailability (i.e. Young's modulus, surface energy, heats of dissolution and solubility). Subsequently, a fundamental understanding of long-range molecular structure is required if we are to make informed decisions during the drug development pipeline. While 'polymorphic form' generally relates to long-range crystal structures, amorphous materials may also be included under this definition and are indeed defined as such in ICH guideline Q6a. The term amorphous generally refers to non-crystalline solids that are disordered (characterised by randomness in their molecular conformation and lack of long-range three-dimensional (3D) orientational symmetry). Interestingly, amorphous solids retain some short-range molecular order which can be similar to that found in crystalline materials [1]. In recent years, amorphous materials have been used due to their substantial solubility advantage and rapid dissolution rate when compared with the corresponding crystalline material [2–4]. However, many concerns, primarily related to stability, arise when using amorphous materials; these include increased chemical instability often as a result of greater hygroscopicity, altered mechanical properties and the possibility of relaxation and/or crystallization during storage [5,6].

The glass transition temperature (T_g) is a characteristic property of amorphous materials [7]. The T_g is the temperature at which an amorphous material changes from a super-cooled liquid with a relatively high viscosity (glass) state to a lower density, lower viscosity (rubbery) state [8]. The T_g is associated with extensive changes in a material's thermodynamic properties such as volume, enthalpy, entropy and heat capacity, and it is characterised by a significant change in molecular motion [8]. At low temperatures, below the T_g, molecular motions are highly restricted to vibrational and short-range rotational motion. As the temperature is increased above the T_g, the molecules become more 'flexible' and mobile resulting in large-scale configurational modification. Subsequently, this increase in molecular mobility above the T_g results in an increase in the volume as a function of temperature [8]. In any particular phase, at equilibrium, the thermodynamic parameters (volume (V), density (ρ), and heat capacity (C_p)) will change relative to temperature. However, as the substance transfers from one phase equilibrium to another, a discontinuity is observed in these parameters, resulting in a different parameter relationship with respect to temperature. For amorphous materials, a plot of

* Corresponding author. Advanced Drug Delivery Group, Faculty of Pharmacy, The University of Sydney, Sydney, NSW 2006, Australia. Tel.: +61 2 9036 7035; fax: +61 2 9351 439.
E-mail address: paul.young@sydney.edu.au (P. Young).

0939-6411/$ - see front matter © 2010 Elsevier B.V. All rights reserved.
doi:10.1016/j.ejpb.2010.12.019

volume or density verses temperature will result in two distinct curves with the intercept being equivalent to the T_g [8,9]. It is important to note, however, that this transition does not involve discontinuous changes in any physical property and thus is not classified as a true phase transition [9]. This phenomenon is illustrated in Fig. 1, where the T_g value usually occurs at around 2/3 of the melting point (T_m) in Kelvin [3,10].

Clearly, an understanding of molecular interaction and 'phase transitions' in API molecules is of great importance to the pharmaceutical sector, since unpredictable changes in a particular solid could result in serious medical implications (i.e. sudden change in bioavailability and formulation failure). Previous studies and theories have generally been empirical in nature; however, with the advancement in high-end computing, the potential to predict and model these phenomena using molecular dynamics (MD) simulation becomes possible. To the authors' knowledge, the application of MD to study phase transitions in small molecule APIs has not been conducted to-date. However, utilising this concept, previous MD simulations have been used to study the T_g of macromolecule polymers with some degree of success [11–18].

This study used MD simulation to model the molecular interactions between a model API, beclomethasone dipropionate, at a range of temperatures. Furthermore, we evaluated the MD approach as a method for determining pharmaceutically relevant physico-chemical parameters. Finally, this approach was correlated with experimentally determined thermal responses using differential scanning calorimetry (DSC) [19].

Beclomethasone dipropionate was chosen as a model drug, since it is an anti-inflammatory corticosteroid for the treatment of chronic asthma [20,21]. In inhalation formulations, the drug must be manufactured with a size conducive to respiratory deposition (i.e. <5 μm). At this scale, the polymorphic form and amorphous stability becomes critical, since small changes in phase will result in highly unpredictable formulation outcomes [22–24].

2. Materials and methods

2.1. Material preparation

Crystalline beclomethasone dipropionate (BDP) was obtained from JAI RADHE SALES (Ahmedabad, India), and analytical grade ethanol was obtained from Biolab (Clayton, Victoria, Australia). Amorphous BDP was obtained by spray drying the supplied BDP from 20% w/v solution in ethanol using a BÜCHI Mini B-290 spray dryer (Flawil, Postfach, Switzerland). Spray drying was conducted using the following settings: feed rate 10 mL min^{-1}, aspiration rate of 100 m^3 h^{-1}, inlet temperatures 60 °C, outlet temperature 38 °C and atomizing pressure 800 kPa. All samples were stored in sealed containers containing silica for a minimum of 48 h prior to use.

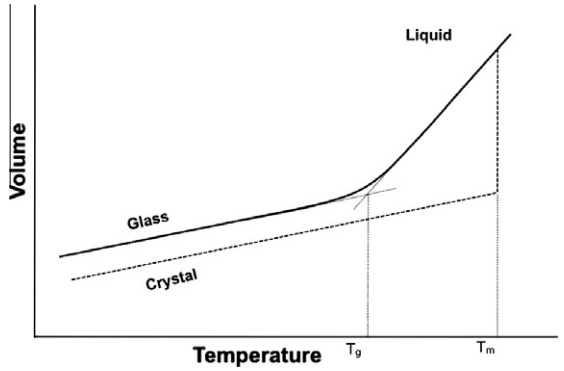

Fig. 1. The relationship between volume and temperature in the liquid, glassy and crystalline states. T_m is the melting temperature, and T_g is the glass transition temperatures.

2.2. Material characterisation

The morphology of the spray-dried amorphous BDP particles was investigated using a scanning electron microscope (SEM) (JEOL 6000F, Japan) at 5 kV. The sample was mounted on adhesive black carbon and sputter-coated with platinum (Sputter coater S150B, Edwards High Vacuum, Sussex, UK) at 40 nm thickness prior to imaging. Amorphous structure was characterised using X-ray powder diffraction (XRD Siemens D5000 diffractometer, Siemens, Karlsruhe, Germany) at a scan range of 5–65°2θ, with step size of 0.05°2θ and a count time of 2 s. The thermal response of the spray-dried amorphous BDP was analysed using a DSC (DSC 823^e, METTLER TOLEDO International Inc.). Samples (ca. 5–8 mg) were crimp-sealed in aluminium sample pans and the lids pierced (to ensure all measurements were conducted under constant pressure). Experiments were conducted at heating rates of 10 and 20 °C min^{-1} over a temperature ramp of 20–280 °C. All DSC measurements were conducted in an inert environment under a nitrogen stream (25 cm^3 min^{-1}). The instrument was calibrated for heat-flow and temperature with a standard indium sample prior to use.

2.3. Computational methodology

Amorphous cell structure prediction and molecular dynamics simulations were performed using Material Studio™ 4.4 (Accelrys Software Inc., San Diego, CA, USA) in a Windows environment. Three-dimensional structural presentations were generated using the Amorphous Cell Module by randomly repeating BDP molecules to a set density within an imaginary cell volume. Initially, two molecules, with the same orientation found in the crystal structure (Fig. 2) [25], were selected and were considered to be the constituent unit for the construction of the amorphous structure. 10, 20 and 30 repeat units (of the two molecules) were used and the three runs yielded amorphous structures containing 20, 40 and 60 BDP molecules, respectively. In subsequent runs, only a single molecule was used with 10, 20 and 30 repeat units (i.e. BPP molecules) being packed into the constructed amorphous cells.

The 3D periodic amorphous cell structures were constructed using an initial density of crystalline BDP (1.36 g cm^{-3} at 298 K) [25]. Twenty amorphous configurations were built during each run using the default construction algorithms. The 3D periodic system parameters were automatically calculated for each run from the number of units used to construct the cell and the target density assuming a cubic cell. A cubic cell was used since previous studies have suggested a cell with equal side lengths is believed to be the optimum shape for calculation, since it would maximize the distance between repeated units in a supercell [26].

Each configuration was minimized using the Discover simulation program. The minimizations were performed under the canonical, NVT, ensemble and were carried out using the Conjugate Gradient method with 1000 dynamic steps and 100 minimization steps. Convergence was set at 0.01 kcal mol^{-1} $Å^{-1}$. The minimized amorphous cell structures from the different runs were visually inspected, and the amorphous cell structures of the single molecule with 30 repeat units were selected for subsequent steps. Of the twenty structures generated from these runs, two with low and medium solvent surface free volume were selected and further optimized. Surface free volume and other properties were calculated with the Models table analysis dialog in Material studio. The geometry of the two selected structures were further optimized using the Forcite Geometry Optimization module with the following settings: COMPASS (Condensed-phase Optimized

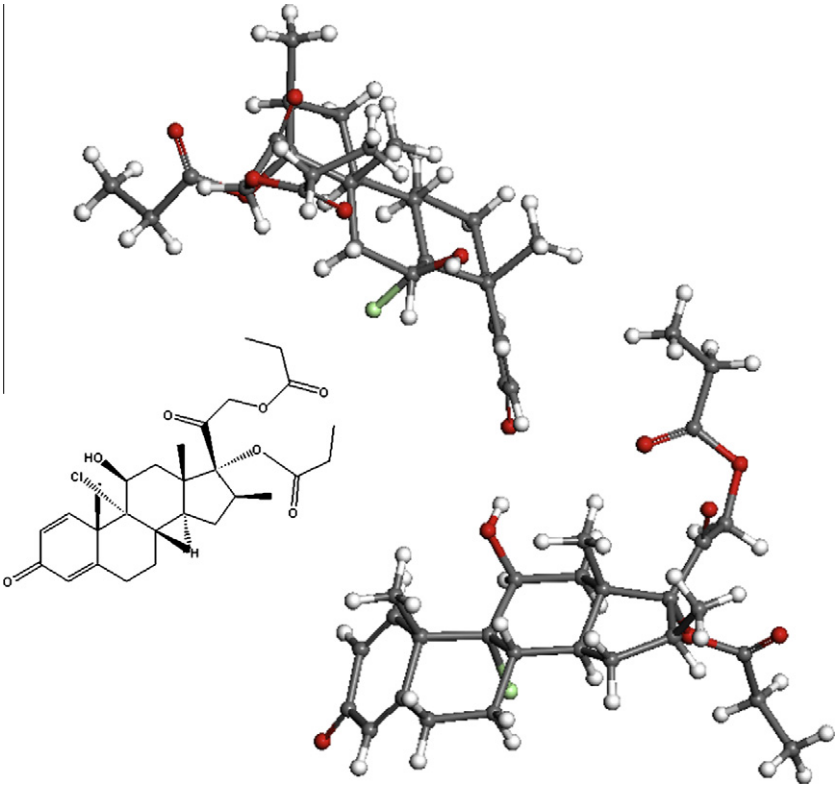

Fig. 2. The conformation of BDP molecules used in amorphous structure prediction, both extracted from the crystal structure and used in the same orientation found in the crystal lattice. (For interpretation of the references to colour in this figure legend, the reader is referred to the web version of this article.)

Molecular Potentials for Atomistic Simulation Studies) [27] force-field; Ewald summation for van der Waals forces; smart algorithm; ultrafine convergence tolerance with 2×10^{-5} kcal mol^{-1} energy variance, 0.001 kcal mol^{-1} Å^{-1} force variance and 1×10^{-5} Å displacement variance and unlimited maximum iterations.

The optimized amorphous cell structures and their unoptimized counterparts were used for MD simulation. The MD simulations were performed on the four structures using Forcite Dynamics, employing the COMPASS force-field at ultrafine quality, while the van der Waals forces were controlled by Ewald summation. The simulations were run under isothermal-isobaric molecular dynamic simulations (MD-NPT) at temperatures between −150 and 400 °C. Temperature was controlled by the Nose thermostat (Q ratio = 1.0). The pressure was maintained at zero with the Berendsen barostat (decay constant = 0.1 ps). Each simulation was run for 25 ps with a 1 fs time step for a total of 25,000 steps.

The simulations were carried out starting from 400 °C and the temperature lowered for each subsequent run. The temperature was initially lowered by 50 °C intervals; however, this was subsequently reduced to 25 °C and 10 °C intervals as the computational temperature approached the theoretical T_g range (based on the known melting point of crystalline BDP). The final optimized amorphous cell structures obtained at each temperature were used as the starting structure for the simulation at the next temperature step.

The values of volume (V) and density (ρ) were obtained directly from the results of each of the four amorphous cell structures simulations. Curves of volume (V) and density (ρ) versus temperature were generated. The temperature at which an abrupt change in the slope was considered to be the simulated glass transition temperature T_g. Curve inflection was calculated by multiple linear regressions of each data set, where the optimum R^2 values above and below theoretical T_g were used and the intercept calculated.

3. Results and discussion

3.1. Physical characterisation

Physical characterisation of the spray-dried BDP was conducted to evaluate particle morphology and molecular structure. Scanning electron micrographs of the spray-dried BDP suggested that the particles exhibited a spherical geometry with a smooth surface, characteristic of amorphous particles (Fig. 3). Furthermore, the particle diameter of the spray-dried BDP was of a suitable size for respiratory drug delivery and thus relevant pharmaceutically. The X-ray powder diffraction patterns of the raw and spray-dried BPP are shown in Fig. 4. The sharp peaks observed in the raw BPD diffractogram indicated a high degree of order, characteristic of a crystalline state. In comparison, the single broad diffuse peak of the spray-dried BDP suggested the material lacked any long-range order (thus confirming its amorphous nature) [10].

The thermal response of the spray-dried BDP, measured by DSC, is shown in Fig. 5. In general, four distinct events were observed over the temperature range 20–280 °C; these corresponded to glass–rubber, rubber–crystal, crystal–melt transitions and thermal degradation, respectively. Furthermore, there was no indication of an endothermic peak corresponding to residual solvent from the spray-drying process (confirmed using thermal gravimetric analysis; data not shown). The endothermic peak at 212 °C followed by an exothermic result indicates the recrystallised BDP undergoes a melt followed by chemical degradation. Furthermore, the spray-dried BDP exhibited an exothermic crystallisation peak at 145 and 150 °C, at heating rates of 10 and 20 °C min^{-1}, respectively. Such observations agree with the previously determined melting and re-crystallisation temperatures of BDP [28]. Crystallisation is considered a kinetically driven transition and thus as the temperature ramp rate increases, the T_g would be expected to shift to a

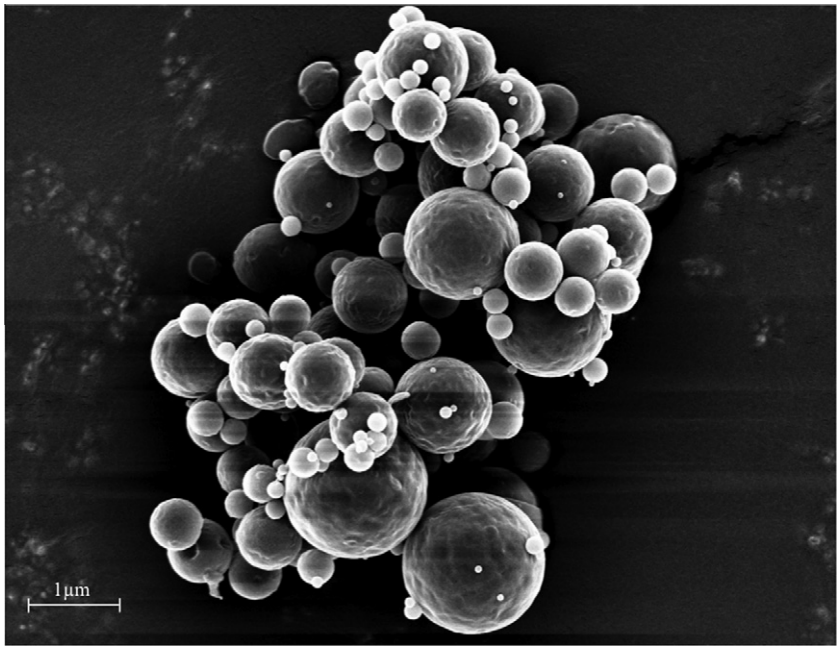

Fig. 3. Scanning electron microscopy of spray-dried BDP.

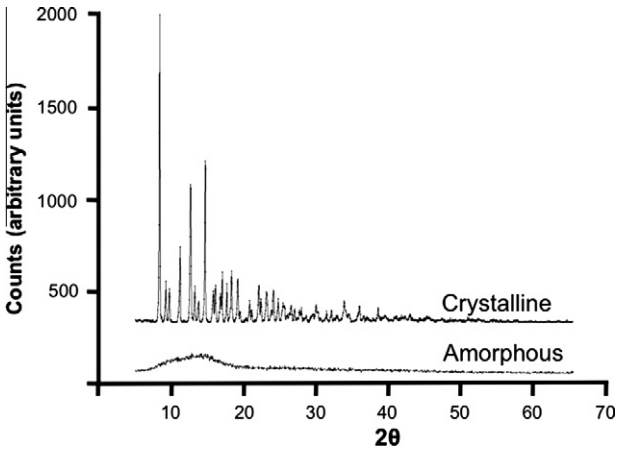

Fig. 4. The X-ray powder diffraction patterns of A: raw (crystalline), and B: spray-dried (amorphous) BDP.

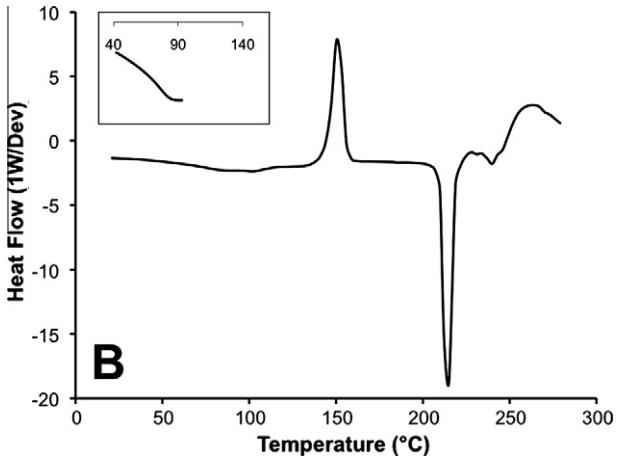

Fig. 5. DSC thermogram of spray-dried BDP at two heating rates of A: 10, and B: 20 °C min^{-1}. T_g is indicated in the boxes (Exothermic: Up).

higher temperature. In comparison, the melting temperature will remain constant, since it is a thermodynamically driven process [29].

In addition to the crystallisation and melting exo/endotherms, an endothermic shift was observed in the baseline between 40 and 80 °C. In general, the glass transition temperature of small pharmaceutical molecules may be predicted from the melting temperature, where the T_g is approximately ~0.7 the T_C (in K) [3,10]. Although such observations are empirical in nature, the T_g for BDP may be estimated as ~66 °C. Analysis of the endothermic baseline shift (Fig. 5 insets) suggests that this estimated T_g value is in good agreement with experimental observation, where analysis of these baseline deflections indicated a T_g of 64.8 and 65.7 °C at 10 °C and 20 °C min^{-1} heating rates, respectively. Again, as it is considered a kinetically driven event, the increase in transition temperature with heating rate is expected.

3.2. Computational modelling

Previous attempts to predict the amorphous structure using random molecules or polymer repeat motifs to construct the amorphous unit cell structures have been conducted [11–15]; however, to date, no such study has focused on pharmaceutically relevant small molecules. Amorphous structure prediction at the molecular level requires special considerations, as the molecular packing of amorphous materials is not related to any crystalline unit cell. Interestingly, it has been shown that the average H-bonding strength in both the amorphous and crystalline forms are uniform, and that a similar pattern of H-bonding may be expected to occur between atoms throughout amorphous structures as observed in their crystalline counterpart [30,31]. In addition, it may be hypothesized that the disordered amorphous materials are expected to retain the molecular packing motif of the corresponding crystalline form but only over very short molecular distances [32]. Subsequently, initial attempts to construct an amorphous structure were conducted with a 2-molecule repeat unit extracted from the crystal lattice reported previously (retaining the different interactions between the molecules) [25]. This was repeated using 10, 20 and 30 units, however, after minimization, the virtual cell resulted in

structures with very low density (i.e. <0.8 g cm^{-3}). It is most likely that the restraints imposed by the presence of two molecules as build units may have affected the spacing of the different molecules within the unit cell upon the amorphous structure construction. Consequently, a single BDP molecule was used for the amorphous structure construction using 10, 20 and 30 molecules. As with the first study, the conformation of BDP as found in the crystal structure was used since, during crystallization molecules tend to acquire low-energy conformations forming optimum H-bonds between the most 'appropriate' H-bond donors and acceptor groups [30]. Interestingly, the generated structure from all three runs showed similar H-bonding patterns (same H-bond donors and acceptor groups) to that observed in the BDP crystal structure; however, the 10 and 20 molecule systems failed to produce compact amorphous structures. It is envisaged that these models did not contain a sufficient number of molecules to sustain an amorphous 'network' and thus the optimized system resulted in discrete molecule clusters separated by void spaces (with densities significantly less than 1 g cm^{-1}). Subsequently, the amorphous cell structures generated from the single 30 unit runs were used in the subsequent simulations.

The analysis of the properties of the twenty generated 30-unit amorphous structures showed that the highest variation was observed in the solvent surface free volume. Upon inspecting three structures with low, medium and high solvent surface free volume, the higher solvent surface free volume cell showed lower packing and therefore was not used in the MD simulation steps.

In addition to the minimization in the amorphous cell construction step, a further optimization was performed on two selected structures to further explore the physico-chemical properties. Upon minimization, more compact structures with closer contacts (H-bond distances and angles) were generated without any other major differences; therefore, all four structures were used for the MD simulations. An example of a minimized and optimized amorphous structure is shown in Fig. 6.

After proceeding with the MD simulations, the four structures resulted in amorphous cells with cell densities above 1 g cm^{-3} with a consistent H-bond network. While an initial cell density of 1.36 g cm^{-3} (cell volume 19085.97 $Å^3$) was used for the amorphous structure prediction (this is equivalent to the crystal density where the free volume is minimized and hence the density is maximized) [30], the optimized cell density was 1.193 ± 0.007 g cm^{-3}. As discussed previously, H-bonds throughout the structure were similar to that of the crystalline counterpart; however, the H-bond distances in the amorphous cell were broad. For example, the H-bond lengths in the 30 unit amorphous models ranged from 1.65 to 2.47 Å with H-bond angles between 108.30° and 178.14°. To put this in perspective, the H-bond angle for crystalline BDP is 2.02 Å with an H-bond angle of 161.13° [25]. Such observations are to be expected, since no long-range structure was observed in the amorphous cell and thus the distance between H-donor and acceptor groups was not fixed.

3.3. Calculation of physico-chemical properties at specific temperatures

In any phase, at equilibrium, the thermodynamic parameters (such as volume, specific volume, density and heat capacity) will change with respect to temperature. The transfer from one phase to another is associated with a discontinuity in this relationship and thus the abrupt change in a curve plotted for any of these parameters versus temperature indicates a change in phase. For amorphous materials, this theory may be utilised for the prediction of the T_g [8,9].

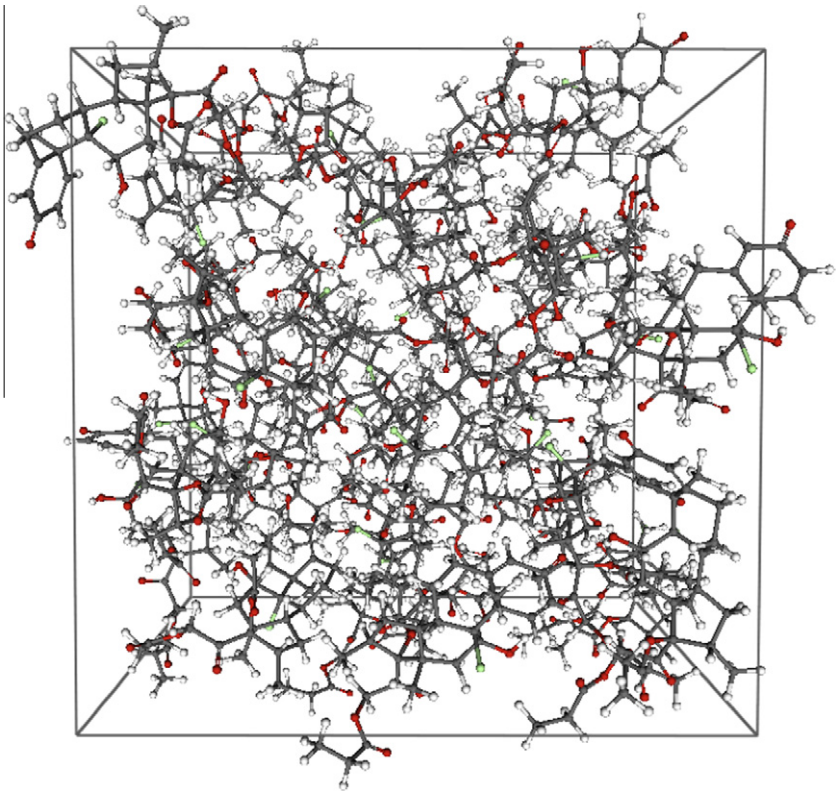

Fig. 6. Amorphous cell structure for BDP constructed using a single BDP molecule. The amorphous cells are composed of 30 repeat units (BDP molecules). (For interpretation of the references to colour in this figure legend, the reader is referred to the web version of this article.)

In MD simulations, the location and velocity vector for each atom can be determined over time within any model structure under a set of specified conditions. The state of the system can be predicted from these positions and velocities and accordingly the system's thermodynamic parameters can be calculated at those conditions. In this study, the MD simulations at isothermal-isobaric conditions were used to determine the different thermodynamic parameters of the modelled systems at each temperature in the range of −100 to 400 °C. The mechanical changes occurring in the system as reflected in the change of volume and density of the systems at different temperatures were monitored. Both parameters showed a discontinuity at around 50–80 °C when plotted versus temperature. A representative data set of the amorphous cell volume and density versus temperature from one of the NPT-MD simulations plotted as a function of temperature are shown in Figs. 7 and 8, respectively, where extrapolation of the intercept resulted in a T_g of 65 °C. Analysis of the four simulations studied here indicated an average T_g of 63.8 ± 2.7 °C. Such observations are in good agreement with the experimental T_g values determined by DSC and theoretical T_g value based on melting temperature.

While this study shows the potential of molecular dynamic simulation for the prediction of the physical properties of amorphous systems, it is important to consider the current limitations and factors which should be considered for further study. Firstly, the process of glass transition is kinetic in nature and therefore variations in T_g at high heating rates should be considered. Furthermore, the current model is not capable of determining high-level phase transitions (i.e. crystallisation), which is observed experimentally, over the temperature range studies here. Finally, when considering more hydrophilic pharmaceutical molecules, the presence of water molecules in the amorphous structure should be considered, since these have a significant effect on the molecular mobility and thus T_g. Ultimately, this approach may be used to determine advanced physico-chemical properties of pharmaceutical systems relative to their formulation (i.e. solubility parameters, surface energy and Young's modulus).

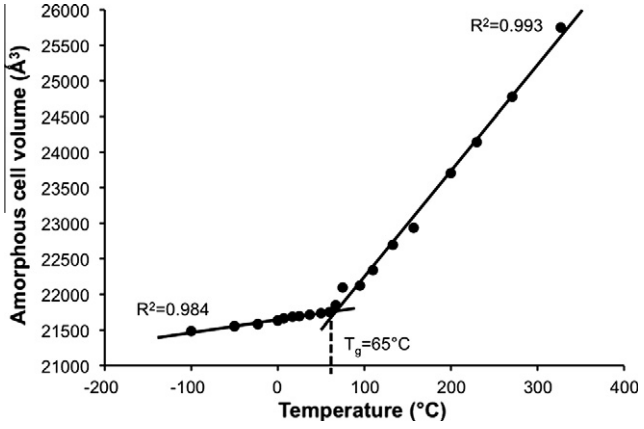

Fig. 7. The change in amorphous cell volume with temperature for BDP amorphous cell structure as estimated from one of the MD simulations.

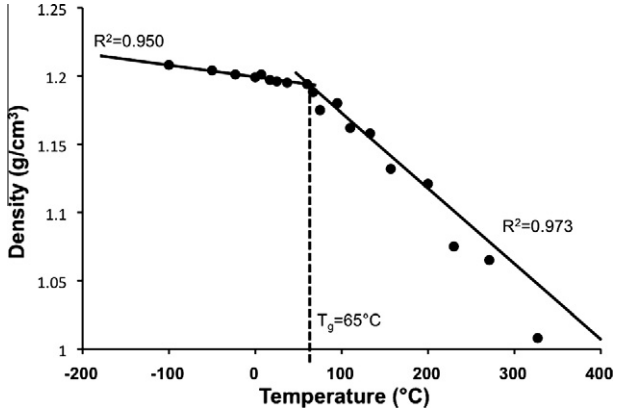

Fig. 8. The change in amorphous cell density with temperature for BDP amorphous cell structure as estimated from one of the MD simulations.

4. Conclusions

Molecular dynamic simulations have been successfully utilised with molecular modelling to estimate the glass transition temperature of polymers. In this work, a similar approach was used to predict the amorphous structure of small, pharmaceutically relevant, molecules and predict their physico-chemical properties. The T_g of BDP was determined by running a series of MD-NPT simulations in the temperature range of −100 to 400 °C. The high agreement between the experimental and predicted T_g values validates the use of this approach to predict the T_g for small molecules. While current solid-state experimental techniques allow rapid and accurate determination of drug T_g, this validated computational approach opens up new avenues for investigating the physico-chemical properties of these systems at the molecular level (for example diffusion properties or the influence of impurities). It is also important to note that this approach was limited to a hydrophobic small drug molecule where future studies should consider amorphous hydrophilic drug systems, where water molecules and, in the case of salts, ionic interactions should be included in the simulation.

Acknowledgements

This research was supported under the Australian Research Council's Discovery Projects funding scheme (Project: ARC-DP0881708). The views expressed herein are those of the authors and are not necessarily those of the Australian Research Council.

References

[1] S.R. Elliott, Medium-range structural order in covalent amorphous solids, Nature 354 (1991) 445–452.
[2] B.C. Hancock, M. Parks, What is the true solubility advantage for amorphous pharmaceuticals?, Pharmaceutical Research 17 (2000) 397–404
[3] D.Q.M. Craig, P.G. Royall, V.L. Kett, M.L. Hopton, The relevance of the amorphous state to pharmaceutical dosage forms: glassy drugs and freeze dried systems, International Journal of Pharmaceutics 179 (1999) 179–207.
[4] L. Yu, Amorphous pharmaceutical solids: preparation, characterization and stabilization, Advanced Drug Delivery Reviews 48 (2001) 27–42.
[5] C.H. Bruno, Z. George, Characteristics and significance of the amorphous state in pharmaceutical systems, Journal of Pharmaceutical Sciences 86 (1997) 1–12.
[6] A.M. Kaushal, P. Gupta, A.K. Bansal, Amorphous Drug Delivery Systems: Molecular Aspects, Design, and Performance 21 (2004) 62.
[7] E. Cernosková, Z. Cernosek, J. Holubová, M. Frumar, Structural relaxation near the glass transition temperature, Journal of Non-Crystalline Solids 284 (2001) 73–78.
[8] P.G. Debenedetti, T.M. Truskett, C.P. Lewis, F.H. Stillinger, Theory of supercooled liquids and glasses: energy landscape and statistical geometry perspectives, Advances in Chemical Engineering, ed., Academic Press, 2001, pp. 21–79.
[9] P.G. Debenedetti, F.H. Stillinger, Supercooled liquids and the glass transition, Nature 410 (2001) 259–267.
[10] B.C. Hancock, G. Zografi, Characteristics and significance of the amorphous state in pharmaceutical systems, Journal of Pharmaceutical Sciences 86 (1997) 1–12.
[11] B.F. Abu-Sharkh, Glass transition temperature of poly(vinylchloride) from molecular dynamics simulation: explicit atom model versus rigid CH_2 and CHCl groups model, Computational and Theoretical Polymer Science 11 (2001) 29–34.
[12] Y. Kun-qian, L. Ze-sheng, S. Jiazhong, Polymer Structures and Glass Transition: A Molecular Dynamics Simulation Study, Macromolecular Theory and Simulations 10 (2001) 624–633.

[13] K.G. Wagner, M. Maus, A. Kornherr, G. Zifferer, Glass transition temperature of a cationic polymethacrylate dependent on the plasticizer content – simulation vs. experiment, Chemical Physics Letters 406 (2005) 90–94.
[14] J. Pozuelo, J. Baselga, Glass transition temperature of low molecular weight poly(3-aminopropyl methyl siloxane). A molecular dynamics study, Polymer 43 (2002) 6049–6055.
[15] D.-X. Li, B.-L. Liu, Y.-s. Liu, C.-l. Chen, Predict the glass transition temperature of glycerol–water binary cryoprotectant by molecular dynamic simulation, Cryobiology 56 (2008) 114–119.
[16] T.A.G. Langrish, Assessing the rate of solid-phase crystallization for lactose: the effect of the difference between material and glass-transition temperatures, Food Research International 41 (2008) 630–636.
[17] N. Dusunceli, O.U. Colak, Modelling effects of degree of crystallinity on mechanical behavior of semicrystalline polymers, International Journal of Plasticity 24 (2008) 1224–1242.
[18] I. Hamerton, B.J. Howlin, P. Klewpatinond, H.J. Shortley, S. Takeda, Developing predictive models for polycyanurates through a comparative study of molecular simulation and empirical thermo-mechanical data, Polymer 47 (2006) 690–698.
[19] M.S. Rahman, I.M. Al-Marhubi, A. Al-Mahrouqi, Measurement of glass transition temperature by mechanical (DMTA), thermal (DSC and MDSC), water diffusion and density methods: A comparison study, Chemical Physics Letters 440 (2007) 372–377.
[20] H.W. Kelly, Comparison of inhaled corticosteroids: an update, Ann Pharmacother 43 (2009) 519–527.
[21] J. Gaddie, I.W. Reid, C. Skinner, G.R. Petrie, D.J.M. Sinclair, K.N.V. Palmer, Aerosol beclomethasone dipropionate in chronic bronchia asthma, The Lancet 301 (1973) 691–693.
[22] P.M. Young, R. Price, The influence of humidity on the aerosolisation of micronised and SEDS produced salbutamol sulphate, European Journal of Pharmaceutical Sciences 22 (2004) 235–240.
[23] C.R. Gardner, C.T. Walsh, O. Almarsson, Drugs as materials: valuing physical form in drug discovery, Nature Reviews Drug Discovery 3 (2004) 926–934.
[24] B.Y. Shekunov, P. York, Crystallization processes in pharmaceutical technology and drug delivery design, Journal of Crystal Growth 211 (2000) 122–136.
[25] J.W. Millard, P.B. Myrdal, Anhydrous beclomethasone dipropionate, Acta Crystallographica Section E 58 (2002) o712–o714.
[26] S.A. Hall, I. Hamerton, B.J. Howlin, A.L. Mitchell, Validating software and force fields for predicting the mechanical and physical properties of poly(bisbenzoxazine)s, Molecular Simulation 34 (2008) 1259–1266.
[27] H. Sun, COMPASS: an ab initio force-field optimized for condensed-phase applications overview with details on alkane and benzene compounds, The Journal of Physical Chemistry B 102 (1998) 7338–7364.
[28] H. Eerikäinen, E.I. Kauppinen, Preparation of polymeric nanoparticles containing corticosteroid by a novel aerosol flow reactor method, International Journal of Pharmaceutics 263 (2003) 69–83.
[29] D.Q.M. Craig, M. Reading, Thermal Analysis of Pharmaceuticals, CRC Press, Boca Raton, 2007.
[30] X.C. Tang, M.J. Pikal, L.S. Taylor, A spectroscopic investigation of hydrogen bond patterns in crystalline and amorphous phases in dihydropyridine calcium channel blockers, Pharmaceutical Research 19 (2002) 477–483.
[31] R.H. Tromp, R. Parker, S.G. Ring, A neutron scattering study of the structure of amorphous glucose, The Journal of Chemical Physics 107 (1997) 6038–6049.
[32] S. Bates, G. Zografi, D. Engers, K. Morris, K. Crowley, A. Newman, Analysis of amorphous and nanocrystalline solids from their X-ray diffraction patterns, Pharmaceutical Research 23 (2006) 2333–2349.